Grant agreement no. 243964

QWeCI

Quantifying Weather and Climate Impacts on Health in Developing Countries

D5.2b: Report on the correlation between malaria observations and meteorological/ecological and environmental variables and correlation between water temperatures and meteorological variables

Start date of project: 1st February 2010 Duration: 42 months

Lead contractor:	UOC
Coordinator of deliverable:	UOC
Evolution of deliverable	
Due date :	M30
Date of first draft :	M36
Start of review :	28 April 2013
Deliverable accepted :	28 May 2013

Project co-funded by the European Commission within the Seventh Framework Programme (2007-2013)		
Dissemination Level		
PU	Public	PU
PP	Restricted to other programme participants (including the Commission Services)	
RE	Restricted to a group specified by the consortium (including the Commission Services)	
CO	Confidential, only for members of the consortium (including the Commission Services)	

Part 1: Report on the correlation between malaria observations and meteorological/ecological and environmental variables

Abstract

This report presents the correlation between meteorological variables and the malaria prevalence in rural peri-urban and urban communities within the Ashanti region of Ghana. In each case, two QWeCI project hospital observations from each community was used and meteorological variables from Ghana Meteorological Agency synoptic stations closest to the hospital locations were used. Children under 5 years and female in the age group of 15–34 were found to have positive malaria cases. Poor positive correlations were found with rainfall in most cases. Negative correlations were seen with temperature for most of the stations in exception of Atonsu, which showed a relatively high positive correlation with temperature.

Introduction

Malaria is one of the most important endemic tropical diseases in Sub-Saharan Africa and it is believed to be responsible for at least one million deaths annually in the world out of which 80% of these deaths occurring in Sub-Saharan Africa (WHO, 2005). Malaria is the leading cause of morbidity in Ghana, accounting for about 37.5% of Out Patients Department (OPD) attendance. Three million six hundred thousand cases of malaria were recorded at the OPDs in the country in 2009. Out of these, 3,900 deaths due to malaria were also recorded during the same period. It is the major cause of death in children under five (5) years (Tay et al. 2012). Malaria therefore has a huge indirect cost on Ghana's economy due to loss of productivity, because those severely infected by malaria are unable to work.

The main vector transmitting malaria in Ghana is the female *Anopheles gambiae* complex and *Anopheles funestus*. *Plasmodium falciparum* is the predominant malaria parasite in Ghana accounting for about 90% of all cases (Tay et al. 2009). Anopheles mosquitoes prefer temporary shallow water for their breeding. However, the stability and productivity of these breeding habitats depend on both the intensity and frequency of rainfall. As high intensity rainfall may flush away breeding larvae, very high storms return periods may not allow full completion of aquatic stage of mosquitos' life cycle.

Malaria prevalence therefore is affected by spatial and seasonal distributions and interannual variability in climate (Cos et al. 2007), and long term trends (e.g. Githeko et al. 2000). Climate variables such as rainfall, temperature and relative humidity have been identified to affect the spread of malaria (e.g. Craig et al. 1999).

This report presents the possible links between climate variability and malaria outpatient cases in some selected hospitals in the Ashanti region of Ghana by determining the relationship between the malaria incidence and climatic variables such as rainfall and temperature.

Climate and Malaria Data Source

The map of the study sites are shown in Figure 1.1. The city quarters Manyia and Atonsu represent urban study sites, whereas, Emena and Ejisu represent peri-urban study sites, and Nkawie and Agogo are used to represent rural community malaria observations. Malaria data for all the six hospitals have been compared with the climate variables. The climate data sources are taken from Kumasi Agromet, Kumasi Airport, as well as from the Owabi and Emena Hospital.

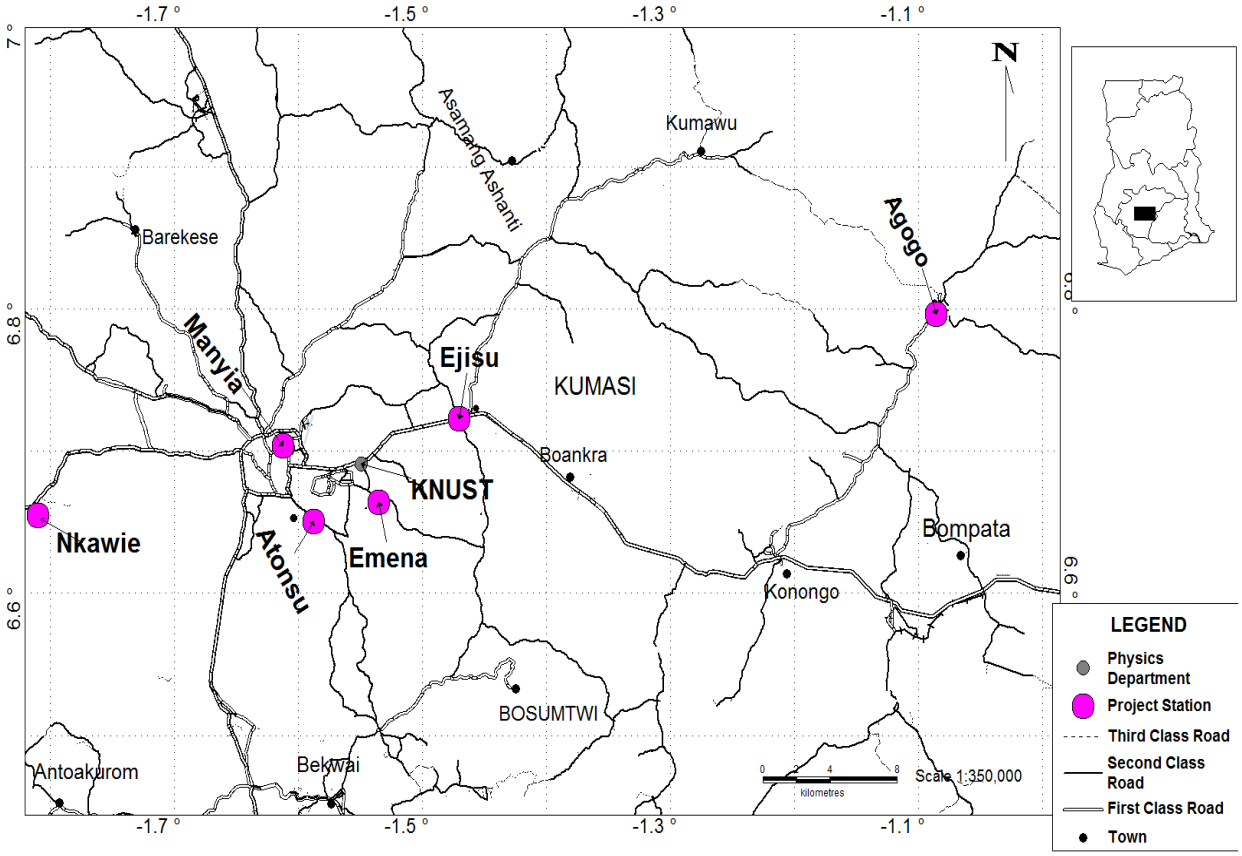

Figure 1.1: *The QWeCI project hospitals (pink shaded circles) in the Ashanti region of Ghana.*

The data collected from the hospitals were grouped according to the World Health Organization (WHO) recommendation. This age grouping therefore provides unequal frequency distribution and hence for statistical meaningful comparison a frequency density was derived using the positive malaria cases reported at the hospital and taking into account the vulnerability relative to each age group within a gender classification. Figure 1.2 shows the outpatient malaria cases reported at the Nkawie hospital between January 2010 and July 2012.

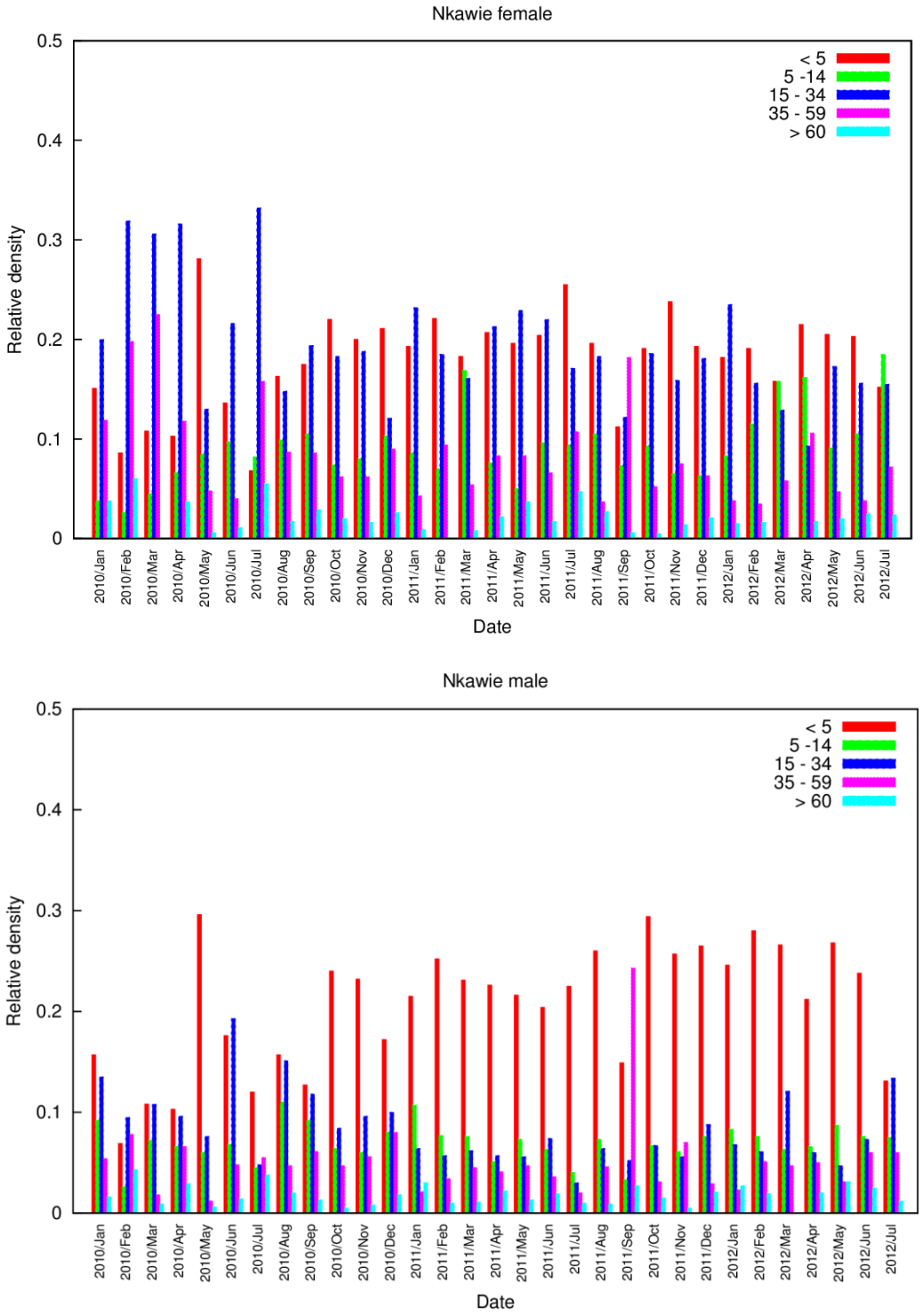

Figure 1.2: *Outpatient malaria cases reported at the Nkawie hospital from January 2010 to July 2012 (Female upper panel and male lower panel).*

A comparison study for age groups was carried out according to a WHO recommendation. In general, the female age group of 15–34 years was found to have persistently high malaria cases. This age group is the most active reproductive period of women and hence these high malaria cases recorded might originate from pregnant women, who are noted to be among the high vulnerability group. Males of ages less than 5 years are also found to have consistently frequent malaria cases. Regarding females, children under 5 years of age were found to be the second most

vulnerable group.

Correlation with climate variables

Rainfall and malaria transmission do not peak at the same time as there is always a time lag between them. The time variation is due to the time required for mosquitoes to complete their life cycle and the parasite to fully develop in the human host. Measured air monthly mean temperatures and monthly precipitation amounts obtained from Kumasi airport synoptic weather station (1.60°W, 6.71°N) were correlated (lag correlation included) with recorded malaria cases from various study hospitals and the results shown in Table 1.1. Weak positive correlations were seen for malaria cases correlated with rainfall for most of the study sites except for Agogo and Ejisu (see Table 1.1). The results shows the deficiency of associating monthly precipitation amount to monthly malaria cases in urban and pre-urban areas where most of the potential breeding habitats are temporary. The stability of this temporary habitat actually depends on intensity and frequency of rainfall events within the month and not on monthly sum. Concerning the lag correlation, it is only Ejisu which has significant correlation coefficient of 0.63 with lag 3 (Table 1.1). With the exception of Atonsu and Agogo, week negative correlation coefficients were observed between monthly mean air temperatures and monthly recorded malaria cases in the other study areas (see Table 1.1). Atonsu shows a positive correlation coefficient of 0.53 and it is the only study area with stable malaria transmission (see Figure 1.6). Agogo shows a strong negative correlation coefficient of -0.79 which may be due to distance between the synoptic weather station and the hospital and using a meteorological data close to the hospital might yield a different results.

Table 1.1: Calculated correlation coefficients for rainfall and temperature and outpatient malaria cases in rural peri-urban and urban hospitals in the Ashanti region of Ghana. The term lag1, lag2,

lag3, and lag4 stand for a lag correlation of 1, 2, 3, and 4 months, respectively.

Correlation Values	Nkawie	Emena	Manhyia	Ejisu	Atonsu	Agogo
Temperature						
Temperature	-0.31	-0.22	-0.21	-0.08	0.53	-0.79
Temperature lag1	-0.26	-0.02	0.00	-0.08	0.36	-0.5
Temperature lag2	-0.19	0.07	0.22	-0.21	-0.07	0.05
Temperature lag3	-0.01	-0.03	0.26	-0.08	-0.33	0.35
Temperature lag4	0.14	-0.15	0.29	-0.12	-0.62	0.63
Rainfall						
Rainfall	0.25	0.24	0.12	0.07	-0.05	-0.01
Rainfall lag1	0.22	0.08	0.11	0.06	-0.22	0.33
Rainfall lag2	0.13	-0.08	0.09	0.63	-0.14	0.25
Rainfall lag3	0.03	0.07	-0.02	0.4	-0.16	0.38
Rainfall lag4	-0.13	-0.01	-0.27	0.09	-0.22	-0.1

It is found from Figures 1.3 that the rainfall and malaria recorded cases are not peaking simultaneously. Increasing rainfall amounts are therefore not leading to an increase in malaria transmission even under the consideration of time lags. This may point to the fact that, most productive breeding habitats are permanent and semi-permanent. This means that rainfall would have a limited effect on malaria cases resulting in a weak correlation coefficient.

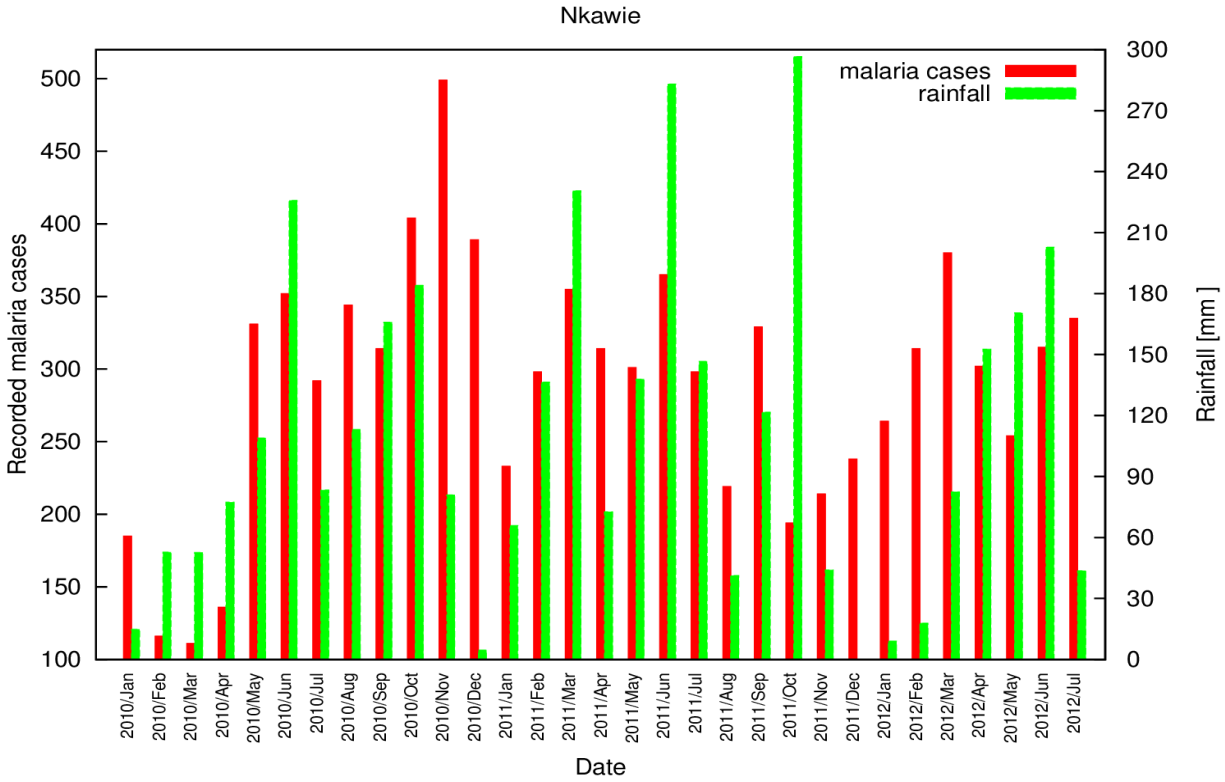

Figure 1.3: *Comparison of rainfall and outpatient malaria cases for Nkawie between January 2010 and July* 2012**.**

Temporary shallow waters are the preferred breeding habitats for *Anopheles gambiae.* These breeding habitats are most productive when there are many rainy days in the month. The critical factors for malaria forecast therefore are the onset and frequency of rainfall since these determine the stability of habitat to complete aquatic stage life cycle. In general, malaria prevalence rate is high in May (see Figure 1.3) because the onset of rainfall in Kumasi is around late March. However, the onset might be delayed sometimes by about a month. At the start of the rainy season rainfall provides additional breeding habitats. This leads to an increase in the Anopheles gambiae mosquito population and hence increases the malaria prevalence.

Malaria in Ghana is hyper endemic with marginal increase in disease incidence during the rainy season. All the climatic factors that influence mosquito breeding and Plasmodium parasite development, precipitation is the only limiting factor as temperatures and relative humidity range are always within malaria transmission range throughout the year. For instance, air temperature decreases during the rainy season, however the temperature recorded during this period are still within the range for mosquito larvae development as well as parasite development in both human and mosquito (see Figure 1.4). Malaria transmission between and within the three study sites (urban, peri-urban and rural) show different trends in recorded malaria cases. Within the urban sites (Atonsu and Manhyia), while Atonsu reveals stable transmission throughout the year, Manhyia on the other hand shows some peaks in recorded cases within the rainy season (see Figure 1.5). The reason for these disparities in recorded malaria cases within these two locations are not known as other factors that impact disease transmission in urban centers are not included

in this study. For instance, the human population size, human activities as urban agriculture impact malaria transmission greatly in Ghana. Results also shows that malaria cases are relatively high in the rural areas as compared to the peri-urban and urban communities (see Figure 1.4), which support the notion that rural dwelling population are at high of malaria than those in urban centers. In addition, comparing malaria cases recorded among males and females, results show clearly that reported cases are high among females than male (see Figure 1.5b and 1.5c). This may be due to that fact that pregnant women, which are vulnerable to malaria infection, are included in the female group.

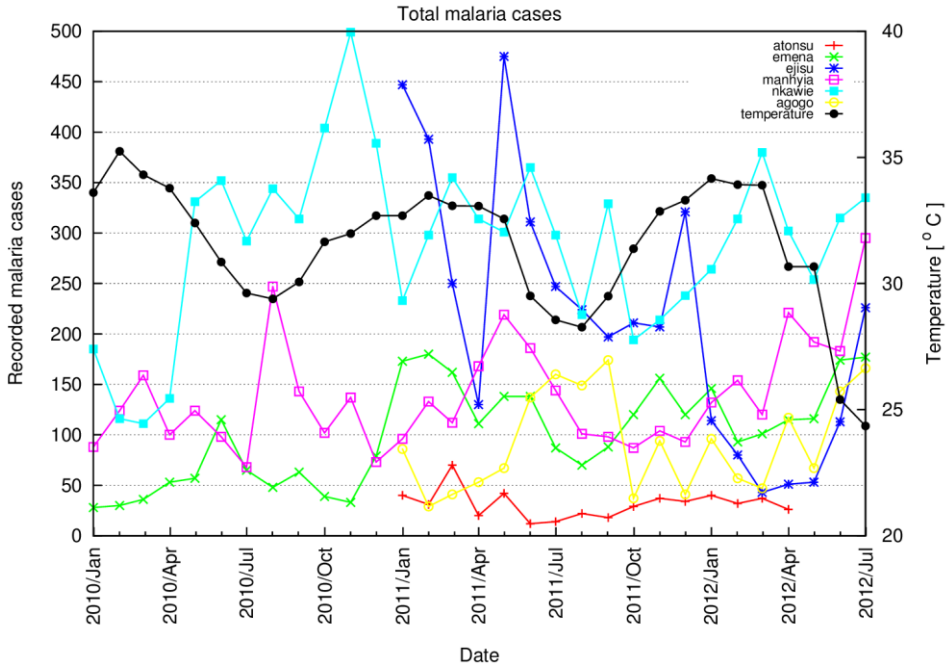

(a)

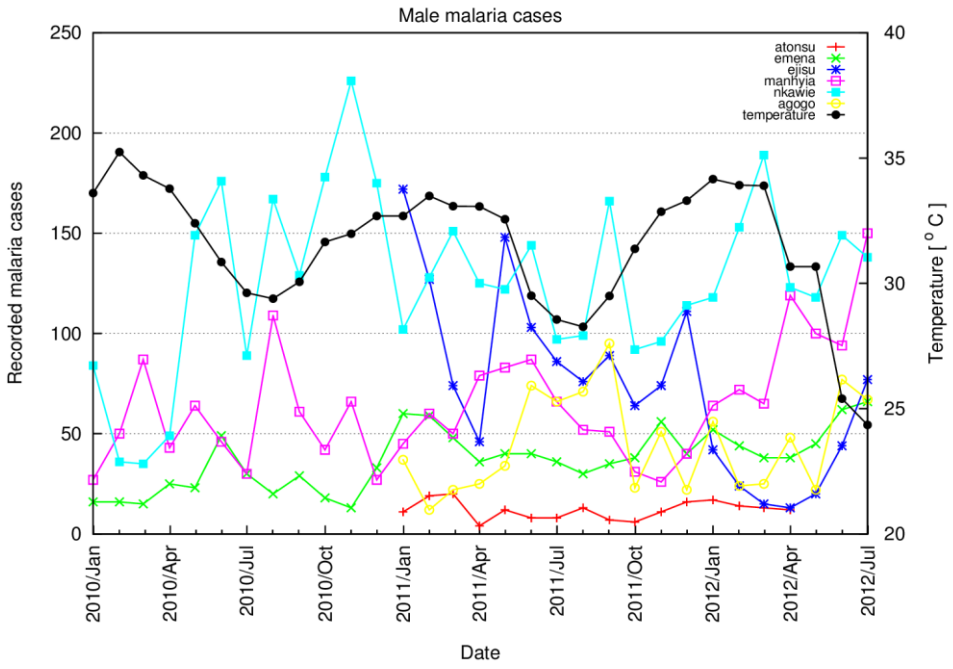

(b)

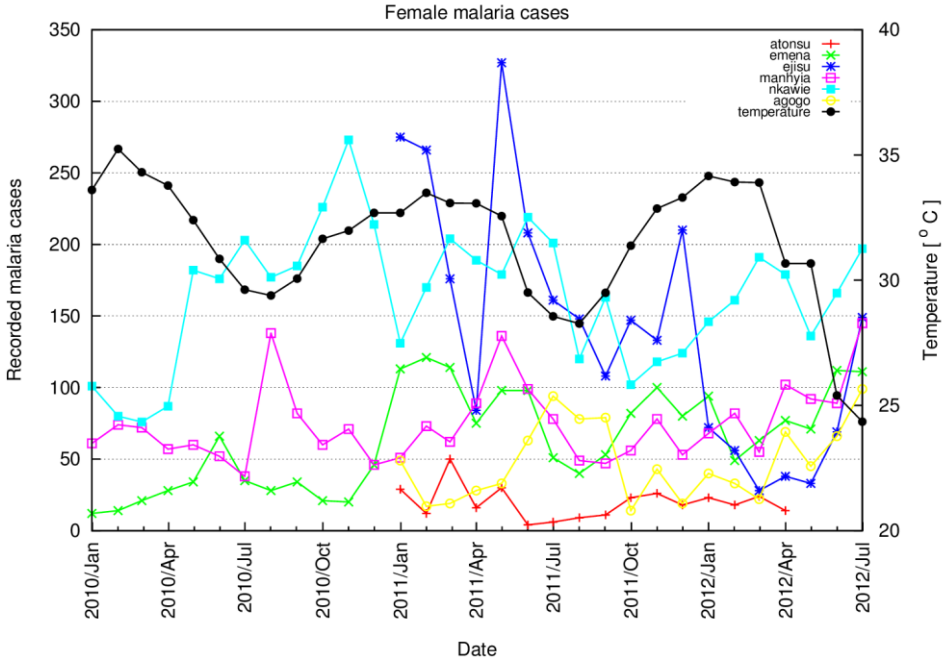

(c)

Figure 1.4: *Comparison of observed monthly temperatures and monthly malaria cases combined for all age groups (a- total, b – male and c - female)*

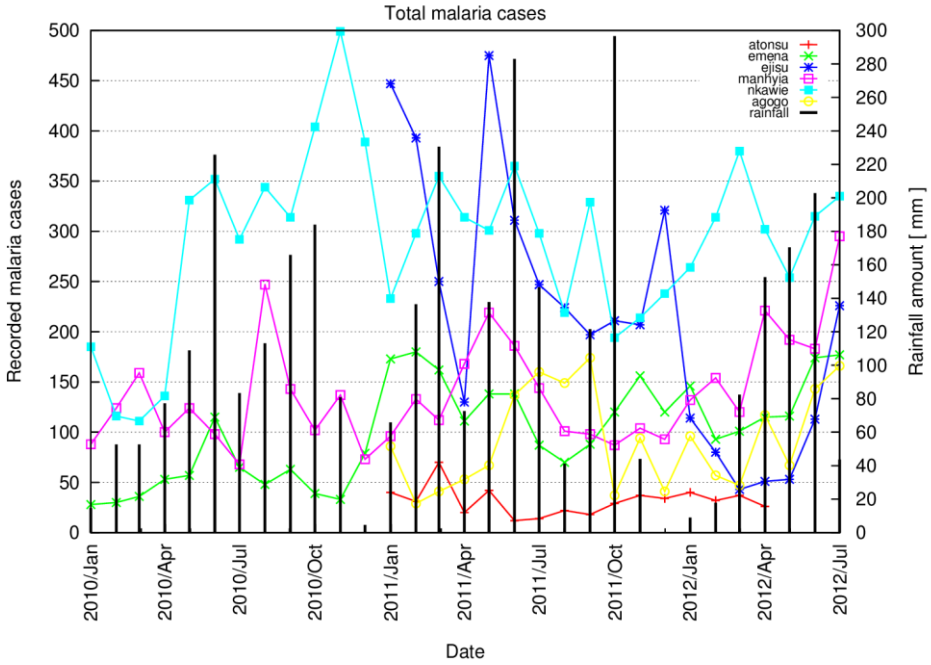

(a)

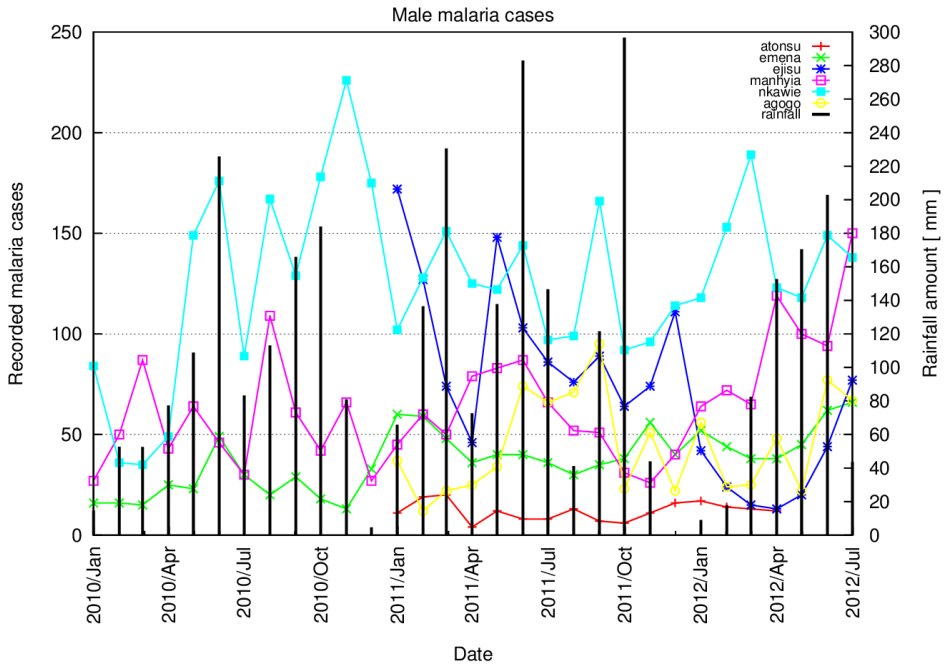

(b)

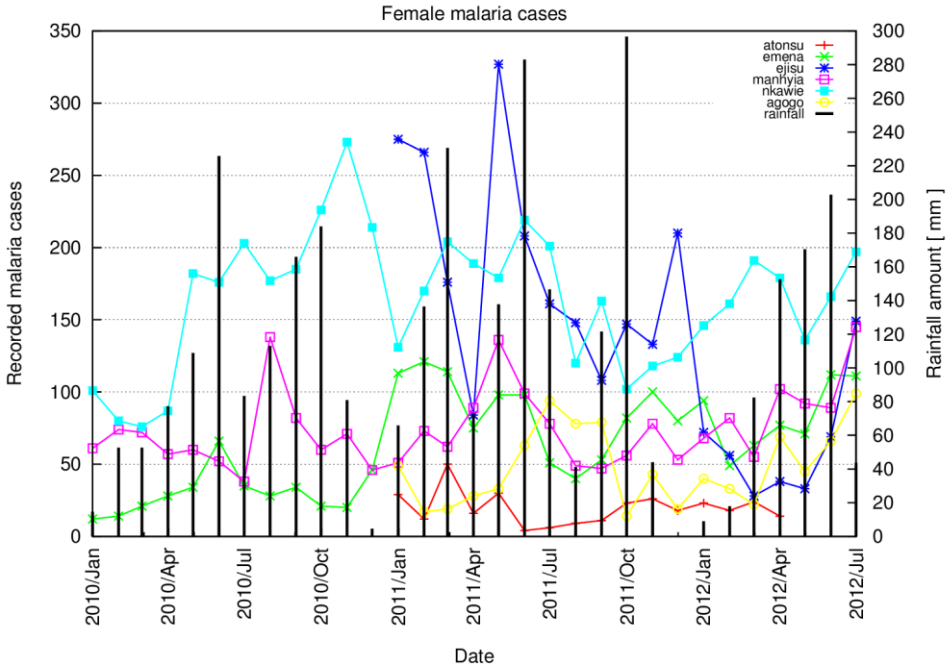

(c)

Figure 1.5: *Comparison of observed monthly rainfall and monthly malaria cases combined for all age groups (a- total, b – male and c - female)*

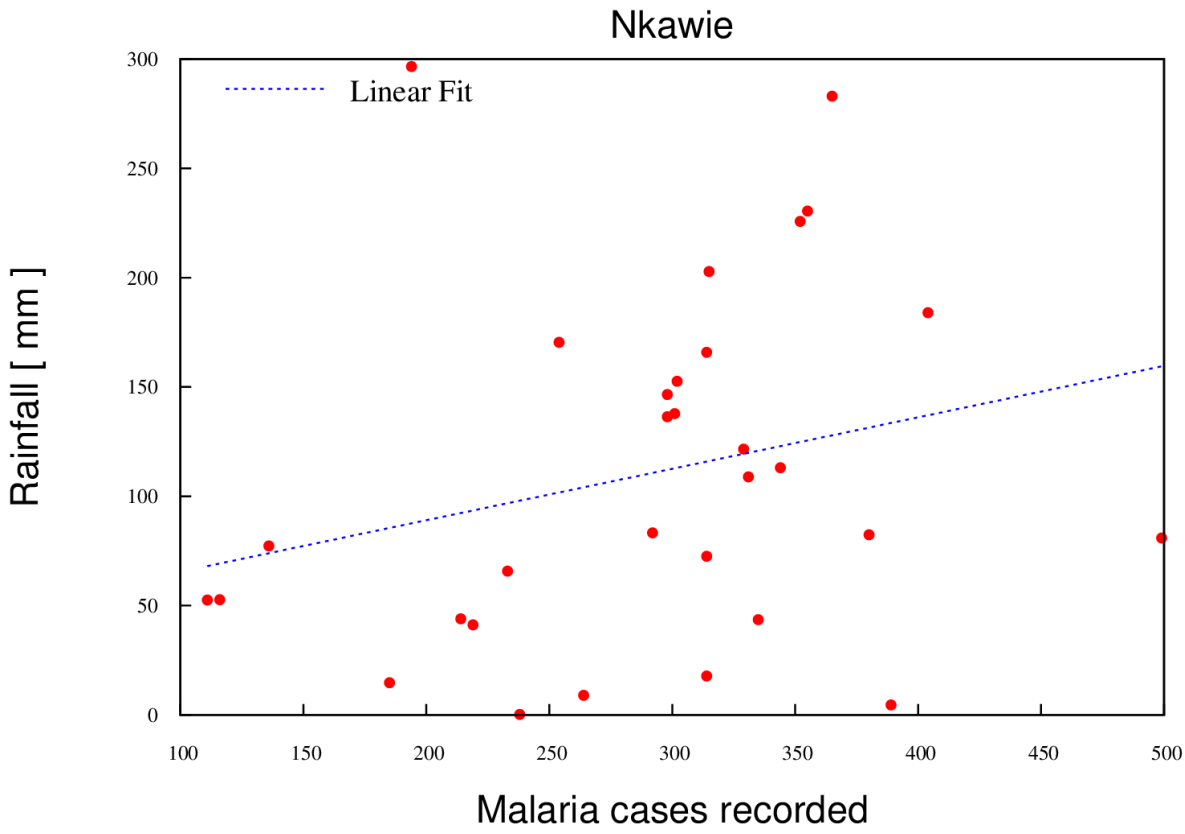

Figure 1.6: *Scatter plot for rainfall as a function of outpatient malaria cases for Nkawie, a typical rural hospital.*

The average monthly temperature for Kumasi is in the range of 25–29°C, which is a favorable temperature for both breeding and survival of mosquitoes. Relative humidity affects malaria transmission by influencing the life span and flight range of Anopheline mosquitoes. The vector has a shorter life span when the relative humidity is below 60%, which may not allow complete development of the parasite within the vector. Results from the monthly data show that throughout the year, relative humidity is greater than 70% and therefore there can be a complete development of the malaria parasite within the vector to increase the probability of infectious bites. This explains the reason for all year round malaria transmission within Kumasi. The limiting factors however are the availability of breeding habitats, which are provided by rainfall, drainage and sewage systems and other environmental factors.

A correlation plot of the temperature with outpatient malaria cases recorded at Nkawie a rural hospital is shown in Figure 1.7. In general, a negative correlation was observed with temperature in most the hospitals (Table 1.1). However, Atonsu hospital located in a poor urban community show a relatively high positive correlation (0.53).

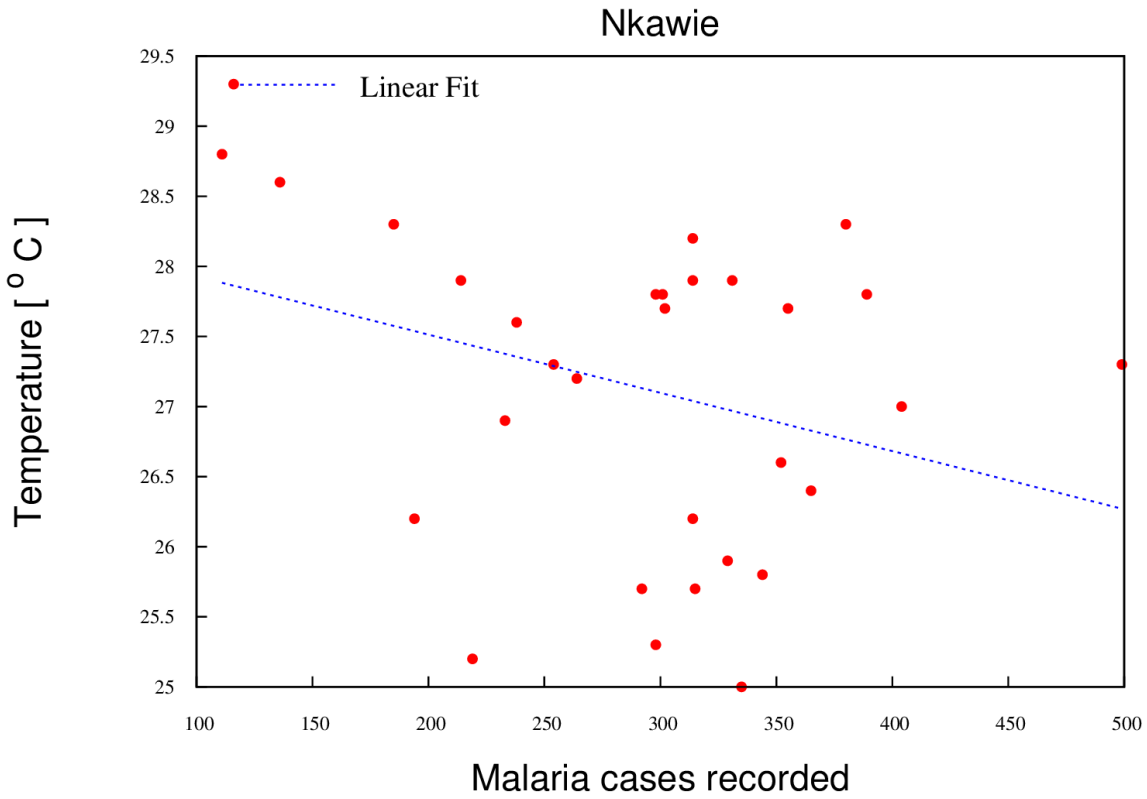

Figure 1.7: *Scatter plot for temperature as a function of outpatient malaria cases for Nkawie.*

Part 2: Correlation between water temperatures and meteorological variables

Abstract

Understanding the interactions between various climatic factors and their combined influence on each stage of the mosquito life cycle is crucial for development of highly skilled early warning system as well as planning of effective control intervention for malaria. Temperature is one important abiotic factor that influences the entire life cycle of mosquitoes and the transmission of malaria. However, present dynamical mathematical-biological malaria models lack a precise simulation water temperatures regarding mosquito breeding habitats as some models simply equate mean air temperatures to water temperatures. Correlation between water temperatures and potential mosquito habitats measured at different times within a day at a peri-urban area of Kumasi (Ghana) and meteorological air temperatures (daily minimum, maximum and mean) from Kumasi airport synoptic station and Owabi automated weather station were assessed. Persistence of temporary breeding habitats was strongly influenced by precipitation. Almost half of the ponds dried out in August 2011 when less rainfall was observed. Pond water temperatures decreased from June to August of about 4°C and the daily water temperatures ranged between about 22 and 36°C. Highest water temperatures were measured during lunchtime (12:00-13:30 UTC). A strong correlation between maximum air temperatures and lunchtime water temperatures were identified with a linear correlation coefficient of about 0.74. The results show the possibility of predicting water temperatures using air temperatures, which is the focus of ongoing work.

Keywords: Africa, Kumasi, malaria, malaria modeling, water temperatures, breeding habitats, ponds, atmospheric temperatures, correlation

Background

The spread of the malaria disease is strongly influenced by weather and climate conditions. Meteorological conditions like atmospheric temperatures, precipitation and humidity conditions and other environmental conditions like water temperatures reveal an impact on malaria transmission. Suitable meteorological conditions for malaria are found along the tropics and the main distribution area of the disease is found in sub-Saharan Africa.

Temperature influences various biological malaria mechanism: (i) the gonotrophic cycle (i.e. the egg development) of mosquitoes takes place only when the temperatures are above about 10°C (Detinova 1962). (ii) The sporogonic cycle is steered by temperatures (e.g. Garrett-Jones and Grab 1964) and the development of the malaria parasite within vectors is only possible above the temperature threshold of about 16°C (Detinova 1962). (iii) Air temperatures impact the vector survival, for instance, temperatures above 40°C strongly reduce the survival probability of mosquitoes (e.g. Kirby and Lindsay 2004). (iv) Larval development depends on water temperatures. For example, Bayoh and Lindsay (2003) showed that Anopheles gambiae sensu stricto emerged as adults only when water temperatures ranged between 18 and 34°C. Most larvae emerged between 22 and 26°C.

At present, dynamical mathematical-biological malaria models lack a precise simulation of water temperatures. For example, Depinay et al. (2004) used the relative humidity to compute cloud

cover and applied the cloud cover to predict maximum air temperatures. By contrast, the minimum water temperature was equated to the minimum air temperature. Tompkins and Ermert (2012) simply equated mean air temperatures to water temperatures in VECTRI (VECtor-borne disease community model of the International Centre for Theoretical Physics, TRIeste). The Liverpool Malaria Model (LMM; Hoshen and Morse, 2003; Ermert et al. 2011a,b) completely neglects the influence of water temperatures on the larval development since the length of the mosquito maturation period is predefined in the model. For this reason, the second part of the study correlates atmospheric temperatures and water temperatures measured in a peri-urban area of Kumasi for a better understanding of the relationship between air temperatures and water temperatures.

Data

Breeding site characteristics in Kumasi. Between 06 June (day 157 in 2011) and 25 August 2011 (day 237 in 2011) daily characteristics of potential mosquito breeding sites were observed in the eastern part of Kumasi. Regularly visited were 15 temporary water bodies within the peri-urban Ayeduase quarter and the KNUST campus of Kumasi (see Figure 2.1).

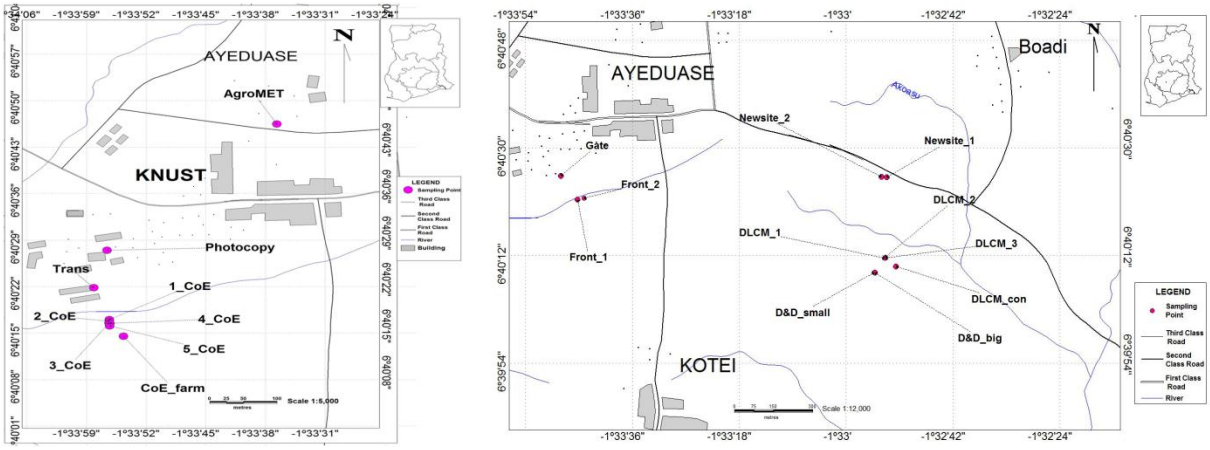

Figure 2.1: *Locations of visited temporary water body sites in the area of the Ayeduase quarter and KNUST campus of Kumasi (see Table°2.1 for more information in terms of the 15 used puddles; source: Ernest Asare).*

The measurements were performed during daylight. Up to three times the water temperatures were measured and once a day in addition the puddle size and depth were observed. Values of the depth were calculated by averaging three different point measurements within the ponds. Noted were also the presence of water and the occurrence of rain (see Figure 2.2 for two typical breeding habitats). The time when the water bodies were visited varied between 07:30 and 16:30 UTC (see Table 2.1). Note that observations were not performed every day during the observational period meaning that some data gaps exist in the time series (see Figure 2.3). The number of potential water bodies decreased over the observational period since various ponds dried out in August 2011. Up to 31 visits per day were undertaken in June 2011, whereas this number decreased to mostly less than 16 visits per day in August 2011, when the number of puddles decreased (see Figure 2.3).

Figure 2.2: *Two typical observed potential mosquito breeding sites in the eastern part of Kumasi.*

In terms of the correlation of measured water temperatures and observed air temperatures, the measurements at the 15 temporary water bodies were combined for four time periods: (i) morning (07:30-09:00 UTC), (ii) late morning (10:00-11:30 UTC), (iii) lunchtime (12:00-13:30 UTC), and (iv) afternoon hours (16:00-16:30 UTC). All measurements within these time spans were averaged for a particular day.

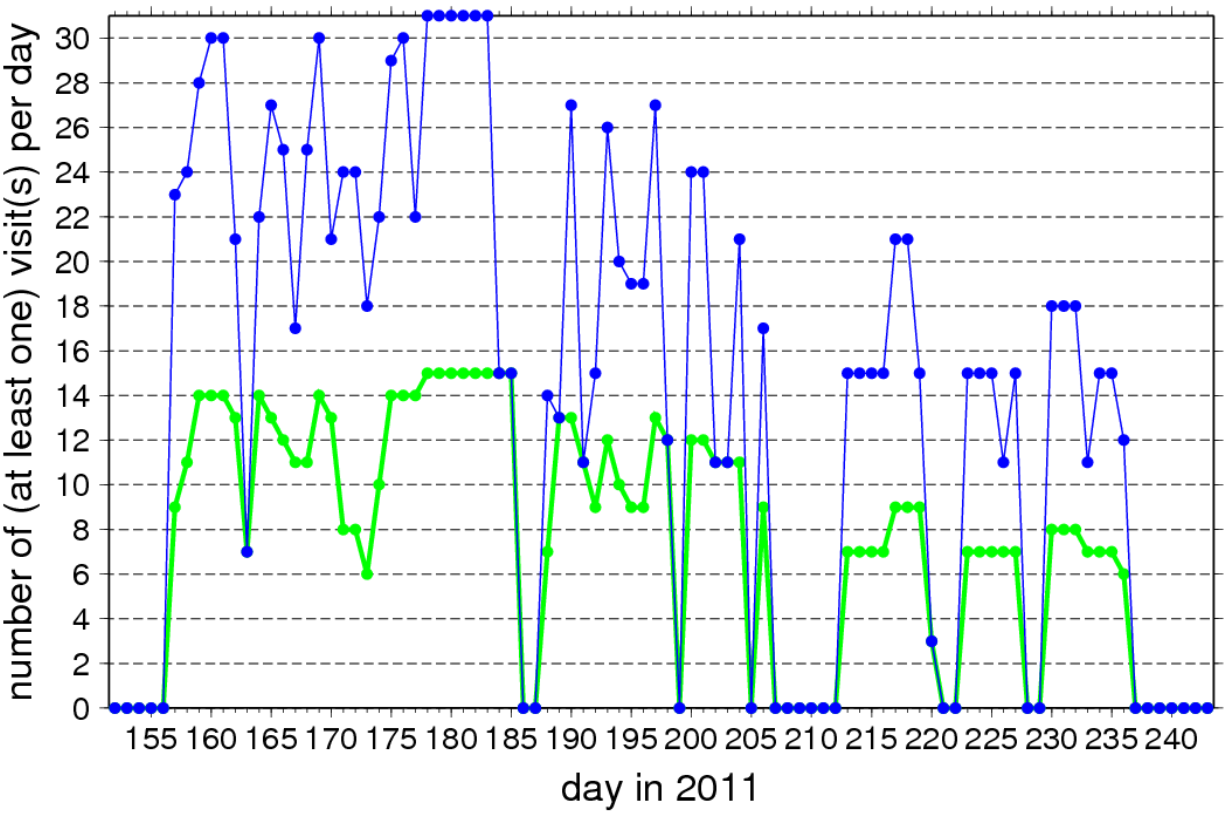

Figure 2.3: *Number of performed temporary water body site observations per day (blue line and dots) and number of at least one visit per water body per day (green line and dots) between June and August 2011.*

Table 2.1: *Latitudinal and longitudinal position, elevation, visiting time, and average dimensions (in cm^2) of the 15 temporary water bodies.*

Number	Name	Longitude	Latitude	Elevation [m]	Visiting time [UTC]	Dimension [cm^2]
1	1_CoE	1°33'56.34''W	6°40'17.04''N	259	10/13/16	23,595
2	2_CoE	1°33'56.30''W	6°40'16.78''N	258	10/13/16	29,948
3	3_CoE	1°33'56.34''W	6°40'16.51''N	257	10/13/16	64,612
4	4_CoE	1°33'56.24''W	6°40'16.48''N	256	10/13/16	60,024
5	5_CoE	1°33'56.28''W	6°40'16.06''N	258	10/13/16	32,691
6	CoE_farm	1°33'54.65''W	6°40'14.52''N	256	10/13/16	14,440
7	Photocpy	1°33'56.60''W	6°40'27.49''N	280	11/13:30/16:30	42,033
8	Trans	1°33'58.15''W	6°40'21.83''N	266	10/13/16	22,359
9	Newsite_2	1°32'54.06''W	6°40'25.15''N	282	07:30/13:30	50,344
10	Newsite_1	1°32'53.18''W	6°40'25.09''N	283	07:30/11:30	115,434
11	DLCM_1	1°32'53.51''W	6°40'11.58''N	259	08:30/12	17,600
12	DLCM_2	1°32'53.38''W	6°40'11.71''N	260	08:30/12	73,407
13	DLCM_con	1°32'51.59''W	6°40'10.14''N	263	08:45/12:15	80,745
14	DLCM_3	1°32'53.41''W	6°40'11.55''N	262	08:30/12	80,745
15	D&D_big	1°32'55.14''W	6°40'09.11''N	268	09/12:15	570,000

Temperature and rainfall observations from Owabi. Air temperatures and precipitation amounts from Owabi/Ghana were extracted from the ***Owabi A****utomatic* ***W****eather* ***S****tation* (**OwabiAWS**) dataset from the QWeCI atmospheric database (http://qweci.uni-koeln.de, go to "Atmospheric database"). The OwabiAWS data includes observations from an **A**utomatic **W**eather **S**tation (**AWS**), which is located at the Owabi hydro-meteorological weather station (1.70289°W, 6.74757°N) in the Kumasi region of Ghana. The weather station but not the AWS is maintained by the Ghana Meteorological Agency.

The OwabiAWS data comprises various observed meteorological variables from the AWS like temperature (***p****latinum resistance* ***t****hermometer*, **PT**100) at a height of 2 m and rainfall (tipping bucket pluviometer). The original temporal resolution of the data was one second and was aggregated or averaged to a time resolution of ten minutes.

From the 10-minutely (10-min) values computed were daily precipitation amounts and temperature values regarding minimum and maximum and daily mean temperatures. The 10-min temperature values were averaged between 06 UTC (actual day) and 06 UTC (following day) for the computation of *daily* ***m****ean* ***t****emperatures* ($\mathbf{T_m}$). At least 80% of the 10-minutely data needed to be present for the calculation of T_m. The ***min****imum* ***t****emperature* ($\mathbf{T_{min}}$) was selected between 18 UTC (previous day) and 06 UTC (actual day). In this case, it was claimed that 80% of the 10-min values were available between 00 and 06 UTC since minimum temperatures in the tropics are in general found in the morning hours. The ***max****imum* ***t****emperature* ($\mathbf{T_{max}}$) was analyzed between 06 and 18 UTC. Here, at least 80% of the 10-min data was needed between 12 and 18 UTC due to the fact that maximum temperatures in the tropics are usually found in the afternoon hours. Note that the ventilation of the temperature sensor broke down partly and that data gaps are present in the three temperature time series (see Figure 2.4). However, only few values are missing in the three temperature time series. Regarding rainfall, all available precipitation measurements were

accumulated for a particular day (06 UTC previous day to 06 UTC actual day) and the number of 10-min data gaps was furthermore noted (Figure 2.5).

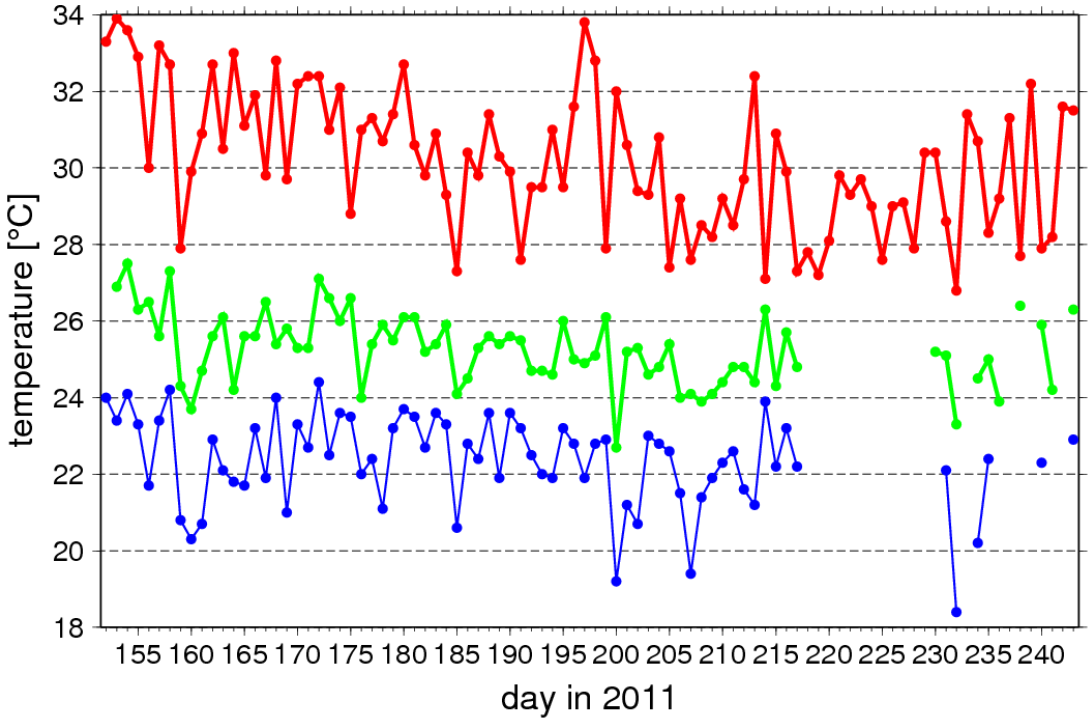

Figure 2.4: *Minimum (blue line and dots), maximum (red line and dots), and daily mean temperature (green line and dots) observations from the OwabiAWS between June and August 2011 (Julian calendar).*

Temperature and rainfall observations from the Kumasi airport. Measured air temperatures and precipitation amounts were also available from the synoptic weather station at the Kumasi airport (1.60°W, 6.71°N; station number of the World Meteorological Organisation: 65442). The station reports with a temporal resolution of 3 hours were downloaded for June to August 2011 from the so-called OGIMET archive (http://www.ogimet.com/synops.phtml.en). Extracted from the so-called SYNOP reports were the 2 m air temperatures as well as minimum and maximum temperatures measured in the Stevenson screen. The 2 m air temperature from Ghana is reported every 3 hours and the values between 09 UTC (actual day) and 06 UTC (following day) were used to compute T_m. At least four of the eight 3-hourly values were required for the calculation of T_m. The minimum temperatures are reported at 06 UTC and are measured between 18 UTC (previous day) and 06 UTC (actual day). Maximum temperature reports are provided at 18 UTC and are measured between 06 and 18 UTC. Due to transmission problems of the SYNOP reports into the ***G****lobal* ***T****elecommunication* ***S****ystem* (**GTS**) not all 3-hourly reports were recorded at the OGIMET database. Altogether 38, 43, and 61 values are missing during the three month period for T_m, T_{min}, and T_{max}, respectively (Figure 2.6).

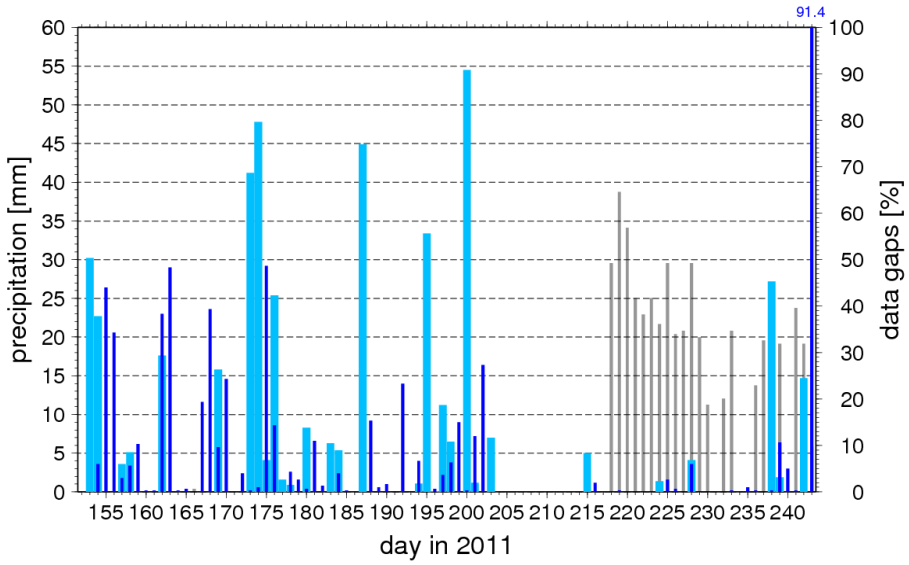

Figure 2.5: *Observed precipitation amounts between June and August 2011 (Julian calendar) at the OwabiAWS (thin dark blue bars) and the synoptic weather station of the Kumasi airport (thick light blue bars). Data gaps (right axis; in percentages per day) of the OwabiAWS are marked by thin dark grey bars (e.g. 25% means that 25% of the 10-minutely AWS measurements are missing).*

Rainfall observations from the Kumasi airport are also available in the SYNOP reports but many data gaps are present between June and August 2011. Altogether 43 of the 24-hour precipitation reports are missing. However, weighing precipitation gauge measurements at the same station are available from the ***Ku****masi* ***P****recipitation* ***Ti****me* ***S****eries* (KuPTiS) data, which is downloadable from the QWeCI atmospheric database (http://qweci.uni-koeln.de, go to "Atmospheric database"). The weighing gauge of the OTT type has a resolution of 0.1 mm of rain and a temporal resolution of one minute. The minutely data was accumulated between 06 UTC and 06 UTC (following day) for the production of 24-hour precipitation amounts (see Figure 2.5).

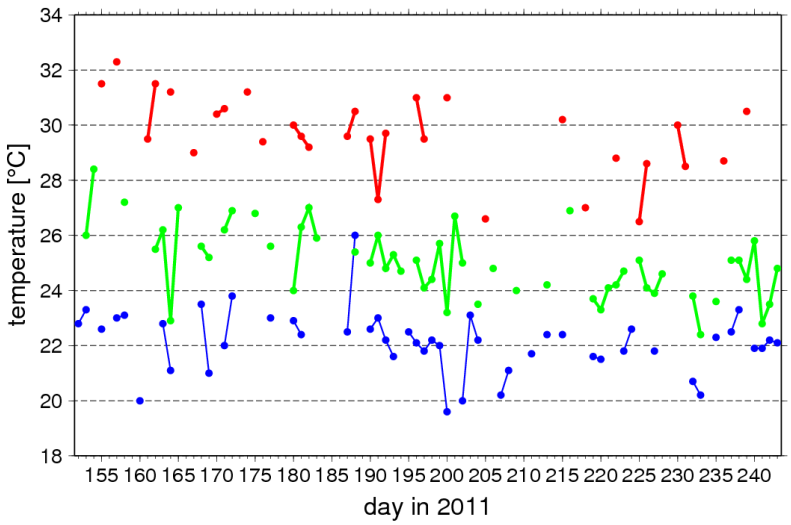

Figure 2.6: *Minimum (blue line and dots), maximum (red line and dots), and daily mean temperature (green line and dots) observations from the synoptic weather station at the Kumasi airport between June and August 2011 (Julian calendar)*

The rainfall observations suffer in terms of artificial rainfall peaks (mostly 0.1 or 0.2 mm of rain in one minute). Therefore, an artificial rainfall filter was used to select realistic rainfall events. Note

that this filter cannot perfectly select precipitation values. Some rainfall events will not be included by the filter and some artificial rainfall peaks will be embedded into the filtered data. Used in this study were the filtered data and not the raw data.

.

Results

Depth and dimension. Average depths of 14 out of the 15 visited temporary water bodies varied between 5 and 11 cm (site 6 is excluded since there was no variation of the water depth). With one exception the deepest depths were observed between the end of June and end of July (Figure 2.7). The averaged dimensions of the visited water bodies (excluded are sites 6, 11, and 15 due to no variation of its size) varied between about 25,000 and 80,000 cm^2 and decreased significantly at the end of the study period. Note that at the end of the observational period only about half of the temporary water bodies were available due to the dry conditions in August (Figure 2.3) and those puddles that were visited rank predominately among the smallest water bodies (Table 2.1). Those puddles existing in August were predominately found in the area of permanent streams. This caused partly the decreased average size of the puddles.

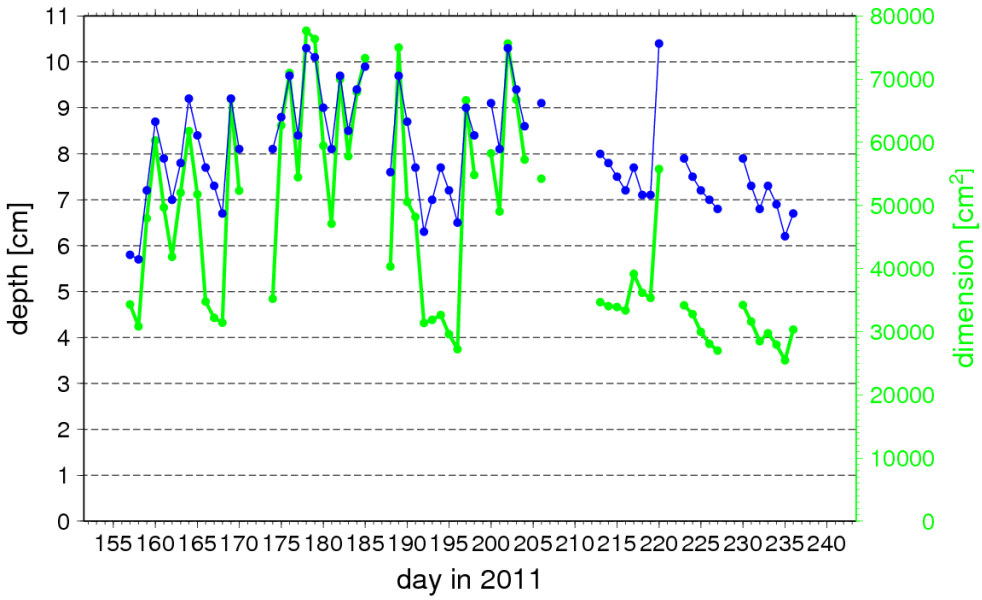

Figure 2.7: *Averaged depth (in cm; site 6 is excluded) and dimension (in cm^2; sites 6, 11, and 15 are excluded) of temporary water bodies within the Ayeduase and Kotei quarters of Kumasi between June and August 2011 (Julian calender).*

The depth and dimension of the water bodies were strongly influenced by precipitation amounts. The rainfall observations from the OwabiAWS and from the Kumasi airport show stronger and more frequently precipitation events in June and July than in August 2011 (see Figure 2.5). This is probably related to the little dry season at the Guinean coast (cf. Vollmert et al. 2004). The rainfall during the West African summer monsoon is usually interrupted at the coastal region during August and September. This is because the lower troposphere is stabilized by cold sea surface temperatures due to an upwelling of cold sea water.

Water temperatures. The averaged water temperatures varied between about 22 and 36°C (Figure 2.8). As expected, the lowest water temperatures were measured during the morning period (07:30-09:00 UTC). During this time the temperatures range between 22 and 28°C. The

highest water temperatures between about 26 and 36°C are found for the lunchtime period (12:00-13:30 UTC), when the sun is at its maximum position. The water temperatures for the late morning (10:00-11:30 UTC) and afternoon (16:00-16:30 UTC) periods are comparable and range between about 25 and 32°C.

It is found that the water temperatures were generally higher during June (days 151-181 in Figures 2.3-2.9) than during July (days 182-212) and August (213-243) (see Figure 2.8). The water temperatures decreased by about 4°C. This fact seems to be partially related to the decreasing air temperatures during about the same time in 2011 (see Figures 2.4 & 2.6).

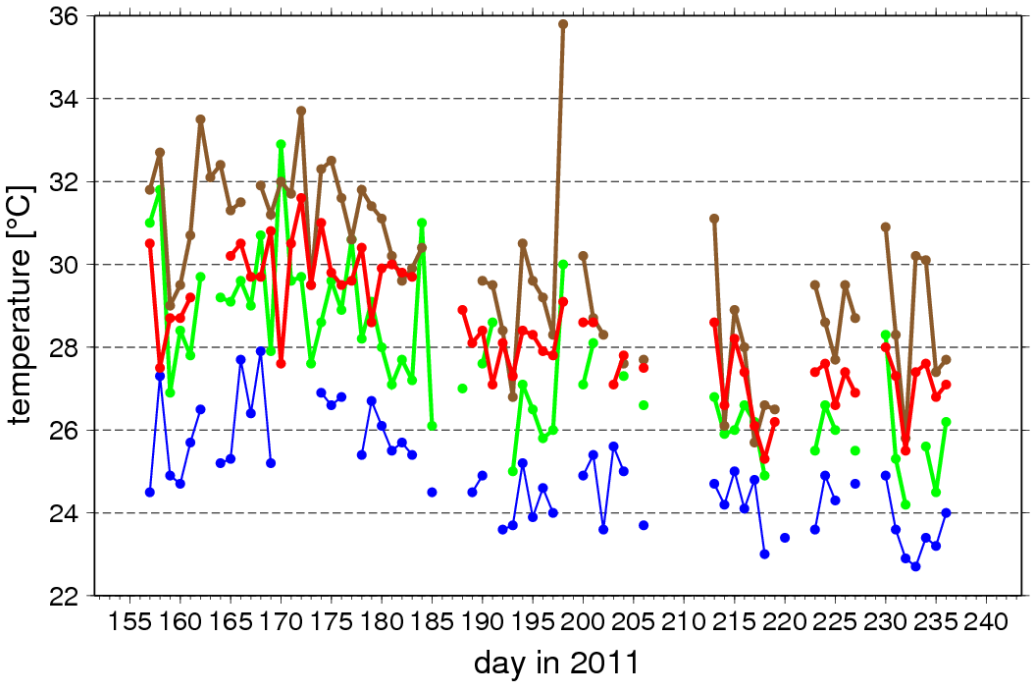

Figure 2.8: *Water temperatures measured between June and August 2011 (Julian calendar) at 15 temporary water bodies within the Ayeduase quarter and KNUST campus of Kumasi during the morning (blue line; 07:30-09:00 UTC), late morning (green line; 10:00-11:30 UTC), lunchtime (brown line; 12:00-13:30 UTC), and afternoon (red line; 16:00-16:30 UTC) hours.*

Correlation of water and atmospheric temperatures. Correlated were the observed water temperatures for different time periods with T_m, T_{min}, and T_{max} measurements at the OwabiAWS and the synoptic weather station of the Kumasi airport (see Table 2.2). As expected, all correlation coefficients are positive meaning that water temperatures rise when air temperatures rise or vice versa. Of course, it is clear from the physical mechanism that the water temperature of temporary water body rise and fall when temperatures are increased and decreased, respectively. The *linear correlation coefficient* (**r**) ranges between about 0.25 and 0.74 meaning that the *coefficient of determination* ($\mathbf{r^2}$) shows values between about 0.06 and 0.55. Note that r^2 provides the proportion of the variance of one variable that is predictable from the other variable. The value of 0.06 would imply that there is no possibility to make predictions of water temperatures. A r^2 value of 0.55, however, means that there is a potential to compute water temperatures from maximum air temperatures.

The highest correlations are found for T_{max} (see Table 2.2 and Figure 2.9). The linear correlation coefficient of T_{max} ranges between values of about 0.40 and 0.74, which transfers to r^2 values between 0.16 and 0.55. The strongest linear correlation is found between T_{max} and water

temperatures measured at lunchtime (see also Figure 2.8). This result is found both for the OwabiAWS and Kumasi airport data. Relatively high linear correlation coefficients of 0.63 and 0.69 are calculated for T_{max} and afternoon water temperatures for OwabiAWS and Kumasi airport, respectively. This result also shows the relative small spatial variation in temperatures. In other words, temperature observations need not to be undertaken very close to the pond measurements.

The T_{min} correlations are highest for observed morning water temperatures, which range between 0.46 and 0.52. As expected, T_{min} explains much better the morning and partly the late morning water temperatures than that at lunchtime or in the afternoon. Note also that positive linear correlation coefficients (0.41-49) are also found for T_{max} and morning water temperatures. This seems to be a result of the thermal capacity of water and the surrounding soil of the water bodies.

Correlations between T_m and water temperatures range altogether between 0.28 and 0.53. With one exception (lunchtime, Kumasi airport) the correlations are smaller than that for T_{max}. In comparison to T_{min}, the T_m correlations are higher in 5 of the 8 cases.

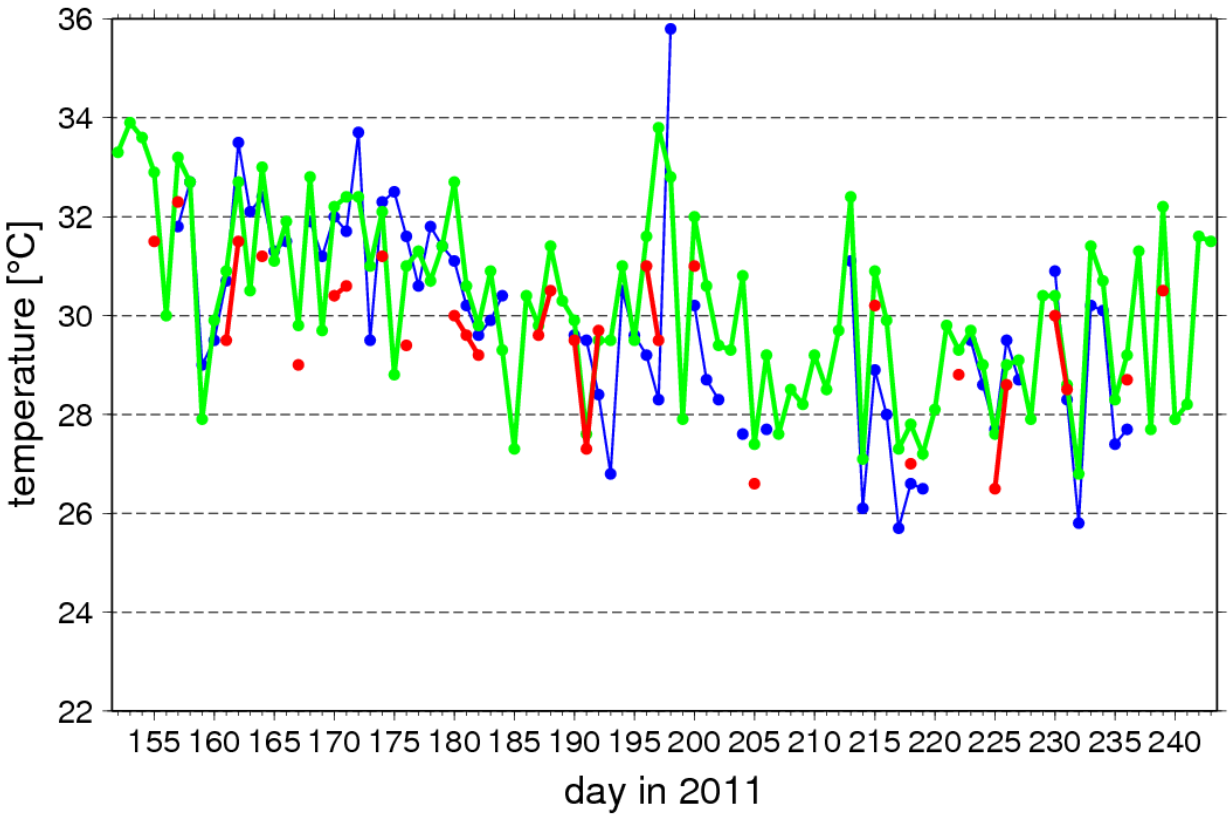

Figure 2.9: *Water temperatures measured between June and August 2011 (Julian calendar) at 15 temporary water bodies within the Ayeduase and Kotei quarters of Kumasi during lunchtime (blue line and dots; 12:00-13:30 UTC) and maximum temperatures measured at the OwabiAWS (green line and dots) and at the Kumasi airport (red line and dots).*

Summary and Conclusions

Water temperature measurements were undertaken in Kumasi between 06 June and 25 August 2011. For the same time period temperature observations (T_m, T_{min}, T_{max}) are available from an

AWS at Owabi and the synoptic weather station of the Kumasi Airport. Most of the visited temporary water bodies revealed a strong variability in terms of the depth, dimension, and water temperatures of the puddles. The depth varied between 5 and 11 cm, the dimension ranged within 25,000 and 80,000 cm^2, and the water temperatures varied between 22 and 36°C. Variability during the day was found for water temperatures with lowest observed water temperatures in the morning and highest measured temperatures at the lunchtime period.

Regarding the correlations of water temperatures and atmospheric temperatures the strongest linear correlation coefficients were discovered for T_{max}. Especially lunchtime water temperatures are highly correlated with T_{max}. In this case, the coefficient of determination (r^2) reveals values up to 0.55. This means that lunchtime water temperatures are to certain extend predictable by T_{max} values. For this reason, it is possible to use T_{max} observations or model results to compute the water temperatures of temporary water bodies. Thus, the present study shows that the of water body temperatures can be used more precisely in dynamical mathematical-biological malaria models.

This study has several limitations since only a short observational period is available and only one study location was used. Moreover, not all temporary water temperatures were visited each day and for each daytime period. Also data gaps are present in the meteorological data, in particular, many synoptic reports are missing for the station at the Kumasi airport. Due to the simple set up of the study, the actual results could be easily reproduced in other malarious locations. Such observations should be predominately performed in the area of weather stations. It would be optimal to measure water temperatures and air temperatures at the same location and with a high temporal resolution. This would require the presence of an AWS and to install a data logger for archiving water temperatures. Note that measurements with a data logger of water temperatures are underway for Kumasi.

Acknowledgements

Ernest Asare is thanked for undertaking the measurements of the pond characteristics. He is currently conducting his PhD at the ***K**wame **N**krumah **U**niversity of **S**cience and **T**echnology* (**KNUST**) working on the hydrology of mosquito breeding sites. Ernest's PhD scholarship was generously funded by two **I**nternational **C**entre of **T**heoretical **P**hysics (**ITCP**) programmes, namely the Italian government's funds-in-trust programme and the ICTP PhD ***S**andwich **T**raining and **E**ducational **P**rogramme* (**STEP**), which enables students from developing countries to spend four months a year at ICTP. ICTP then used QWeCI funds to extend the exchange period to 6 months.

Table 2.2: *Linear correlation coefficients (r) between water temperatures measured at 15 temporary water bodies within the Ayeduase quarter and KNUST campus of Kumasi at different time periods (see text) and 2 m screen temperatures (T_m, T_{min}, T_{max}) observed at the OwabiAWS (***bold figures***) and the synoptic weather station of the Kumasi airport (italic figures). The numbers in brackets display the number of available observations.*

Visiting time	Air temperature	Linear correlation coefficient
morning	T_{min}	**0.466 (45)**
(07:30-09:00 UTC)		*0.518 (27)*
	T_m	**0.435 (47)**
		0.531 (31)
	T_{max}	**0.494 (54)**
		0.406 (21)
late morning	T_{min}	**0.441 (50)**
(10:00-11:30 UTC)		*0.284 (28)*
	T_m	**0.440 (52)**
		0.458 (33)
	T_{max}	**0.575 (57)**
		0.501 (24)
lunchtime	T_{min}	**0.315 (50)**
(12:00-13:30 UTC)		*0.348 (32)*
	T_m	**0.381 (52)**
		0.284 (38)
	T_{max}	**0.736 (60)**
		0.738 (24)
afternoon	T_{min}	**0.249 (49)**
(16:00-16:30 UTC)		*0.287 (31)*
	T_m	**0.435 (51)**
		0.507 (35)
	T_{max}	**0.631 (59)**
		0.688 (24)

References

Bayoh MN, Lindsay SW, 2003: Effect of temperature on the development of the aquatic stages of Anopheles gambiae sensu stricto (Dipteria: Culicidae*). Bull Entomol Res,* **93:**375-381.

Depinay J-MO, Mbogo CM, Killeen G, Knols B, Beier J, Carlson J, Dushoff J, Billingsley P, Mwambi H, Githure J, Toure AM, McKenzie FE, 2004: A simulation model of African Anopheles ecology and population dynamics for the analysis of malaria transmission. *Malar J,* **3:**29.

Detinova TS, 1962: Age-grouping methods in Diptera of medical importance with special reference to some vectors of malaria. WHO, Monograph Series No. 47, 216 pp.

Ermert V, Fink AH, Jones AE, Morse AP, 2011a: Development of a new version of the Liverpool Malaria Model. I. Refining the parameter settings and mathematical formulation of basic processes based on a literature review. *Malar J,* **10:**35.

Ermert V, Fink AH, Jones AE, Morse AP, 2011b: Development of a new version of the Liverpool Malaria Model. II. Calibration and validation for West Africa. *Malar J,* **10:**62.

Garrett-Jones C, Grab B, 1964: The Assessment of Insecticidal Impact on the Malaria Mosquito's Vectorial Capacity, from Data on the Proportion of Parous Females. *Bull WHO,* **31:**71-86.

Hoshen, M. B., and A. P. Morse, 2004: A weather-driven model of malaria transmission. *Malar J*, **3:**32.

Tompkins AM, Ermert V, 2012: A regional-scale, high resolution dynamical malaria model that accounts for population density, climate and surface hydrology. Submitted to *Malar J.*

Vollmert P, Fink AH, Besler H, 2003: Ghana- und Dahomey-Trockenzone: Ursachen für eine Niederschlagsanomalie im tropischen Westafrika. *Erde,* **134:**375-393.

Cox, J, SI. Hay SI, Abeku A , Checci F, Snow RW, 2007: The uncertain burden of Plasmodiumfalciparum epidemics in Africa. *Trends Parasitol,* **23:**142-148.

Craig MH, Snow RW, le Suer D, 1999: Climate based Distribution Model of malaria Transmission in Sub-saharanAfrica. *Parasitol Today,* **15:**105-111.

Tay SCK, Danuor SK, Mensah DC, Acheampong G, Abruquah HH, Morse A, Caminade C, Badu K, Tompkins A, Hassan HA, 2012: Climate variability and malaria incidence in peri-urban, urban and rural communities around Kumasi, Ghana: A case study at three health facilities Emena, Atonsu, and Akropong. *International Journal of Parasitology Research,* **4:**83-89.

Githeko AK, 2009: Malaria and Climate Change. In: Commonwealth Health Ministers' Update 2009. Published for the Commonwealth Secretariat by Pro-Brook Publishing Limited, pages 42-45.

Tay SCK, Danuor SK, Morse A, Caminade C, Badu K, Abruquah HH, 2012: Entomological survey of malaria vectors within the Kumasi metropolitan area – A study of three communities: Emena, Atonsu and Akropong. *Journal of Environmental Science and Engineering,* **1:**144-154.